

Novel Rubidium Poly-Nitrogen Materials at High Pressure

Ashley S. Williams,¹ Brad A. Steele,¹ and Ivan I. Oleynik^{1, a)}

Department of Physics, University of South Florida, Tampa, FL 33620

First-principles crystal structure search is performed to predict novel rubidium poly-nitrogen materials at high pressure by varying the stoichiometry, i. e. relative quantities of the constituent rubidium and nitrogen atoms. Three compounds of high nitrogen content, RbN_5 , RbN_2 , and Rb_4N_6 , are discovered. Rubidium pentazolate (RbN_5) becomes thermodynamically stable at pressures above 30 GPa. The charge transfer from Rb to N atoms enables aromaticity in cyclo- N_5^- while increasing the ionic bonding in the crystal. Rubidium pentazolate can be synthesized by compressing rubidium azide (RbN_3) and nitrogen (N_2) precursors above 9.42 GPa, and its experimental discovery is aided by calculating the Raman spectrum and identifying the features attributed to N_5^- modes. The two other interesting compounds, RbN_2 containing infinitely-long single-bonded nitrogen chains, and Rb_4N_6 consisting of single-bonded N_6 hexazine rings, become thermodynamically stable at pressures exceeding 60 GPa. In addition to the compounds with high nitrogen content, Rb_3N_3 , a new compound with 1:1 RbN stoichiometry containing bent N_3 azides is found to exist at high pressures.

I. INTRODUCTION

Poly-nitrogen materials are being actively investigated¹⁻⁶ with the goal to obtain stable high-nitrogen content compounds, which are expected to outperform conventional all-organic energetic materials (EMs). The pure single-bonded cubic gauche (cg) polynitrogen crystal⁷ would be the leading candidate, as the decomposition of the single-bonded condensed-phase nitrogen to the gas-phase triple bonded diatomic N_2 molecules results in enormous release of energy. In 2004, Eremets *et al.*⁸ successfully synthesized the single-bonded cg phase of polymeric nitrogen, that was originally predicted to be energetically favorable over the epsilon phase of N_2 above 50 GPa⁹. In 2014, Tomasino *et al.*¹⁰ discovered a new layered polymeric phase of nitrogen. Unfortunately, the synthesis of polymeric nitrogen requires excessive heating above 2000 K and enormous pressures above 100 GPa. Moreover, its recovery at ambient conditions is challenging¹¹. For this reason, new approaches for the synthesis of high nitrogen content materials are urgently sought^{1-3,6,12-14}.

Introduction of other elements into polynitrogen-containing crystals appears to be a viable route to promote metastability while reducing synthesis pressure^{12,13,15}. Previously, alkali polynitrogen materials including sodium¹³, cesium^{12,16}, and lithium¹⁷ polynitrides have been investigated at high pressures. In particular, cesium pentazolate CsN_5 , consisting of pentazolate N_5^- anions and Cs^+ cations was predicted, and then synthesized¹². The presence of alkali metal atoms facilitates the electron transfer to nitrogen N_5 clusters, thus making cyclo- N_5^- aromatic. Previously studied alkali nitrides XN_y , $\text{X} = \{\text{Cs}, \text{Na}, \text{Li}, \text{K}\}$ display similarities: some of them contain N_5 pentazolates at a specific stoichiometry XN_5 or infinite nitrogen chains in XN_2 stoichiometry^{12,13,16-18}. First-principles calculations show that cesium pentazolate^{12,16} and lithium

pentazolate¹⁷ are stable above 15 GPa whereas sodium pentazolate is predicted to be stable above 20 GPa. The cesium pentazolate material was synthesized in a diamond anvil cell by compressing and laser heating CsN_3 and N_2 to pressures near 60 GPa¹². High-nitrogen compound X_4N_6 containing N_6 hexazine rings is predicted to exist in the case of cesium and potassium, whereas no such structures are found in case of Li_xN_y and Na_xN_y materials^{12,17,18}.

Based on the similarities and differences between alkali polynitrides, the interesting question is whether rubidium pentazolate exists and whether it could be synthesized under similar conditions as CsN_5 using possible precursor mixture, $\text{RbN}_3 + \text{N}_2$. The barrier to decomposition of cyclo- N_5^- into $\text{N}_3^- + \text{N}_2$ is significant, 92 kJ/mol. Therefore it is expected to be metastable at ambient conditions making it a promising candidate for high nitrogen content EMs.^{19,20} The relative stability of cyclo- N_5^- allowed the synthesis of cyclo- N_5^- compounds at ambient conditions.²¹⁻²⁴

In this work, rubidium polynitrogens are investigated with the goal to explore novel polynitrogen EMs. Being similar to cesium, rubidium polynitrogens are interesting as for both elements, d electrons of the core begin to play a prominent role at high pressures. An indirect indication of the expected diversity in rubidium polynitrogen compounds is the complex phase diagram of pure Rb, which possesses six phases between 0 and 48 GPa^{25,26}. This is in contrast to Na that has only two stable phases between 0 GPa and 100 GPa with the phase transition from bcc to fcc occurring at sufficiently high pressure 60 GPa²⁷. It is suggested that the presence of occupied $3d$ orbital results in destabilization of the bcc and fcc structures at high pressures²⁵. The goal of this work is to predict and characterize new rubidium polynitrogen materials, including but not limited to RbN_5 and RbN_2 , as well as to discuss future experimental realization of our predictions by suggesting possible precursors and corresponding pressures to initiate the high pressure chemistry.

^{a)}Electronic mail: oleynik@usf.edu

II. COMPUTATIONAL METHODS

A search for new compounds of varying Rb_xN_y stoichiometry is performed using the first-principles evolutionary structure prediction method USPEX²⁸⁻³⁰ at four pressures, 0, 30, 60 and 100 GPa. For each pressure the search begins by generating crystal structures containing variable amounts of elemental rubidium and nitrogen with 8 - 16 atoms in the unit cell. The crystals in the first generation are built with a random composition and lattice parameters. Density functional theory (DFT) is then used to minimize the total energy at fixed hydrostatic pressure by relaxing the atomic coordinates and the unit cell parameters of each structure of the entire population. The structures are then ranked by their formation enthalpy, those with the lowest formation enthalpy being the most favorable. A new generation of crystals is then produced with a combination of the lowest enthalpy structures from the previous generation, new random structures, and by applying variation operators, such as atom mutations and lattice permutations, to the lowest enthalpy structures to make a set of new crystals. This cyclic process of creating and optimizing new generations repeats until the best structures do not change for the last ten generations.

If applied properly, the USPEX method is very robust. In particular, we search for 99 compositions of Rb_xN_y over a wide range of pressure. Taking into account such an exhaustive set of stoichiometries and the relative simplicity of the chemistry of the binary compounds, it is very likely the method found all the important compounds consisting of a reasonable number of atoms per unit cell. In two cases, a molecular search was also conducted in addition to the standard USPEX variable composition search to determine if larger crystals would lower the enthalpy compared to the smaller molecular crystals that were found during the variable composition search.

The convex hull, a formation enthalpy versus composition plot, is generated to determine which compounds are thermodynamically stable. The convex hull is constructed with the lowest formation enthalpy phases of each compound. If the compound lies on the convex hull, it is considered thermodynamically stable³¹ and will not decompose into the constituent pure elements or other Rb_xN_y compounds. The formation enthalpy is defined as the difference in enthalpy of a given compound and the sum of the enthalpies of the pure referenced structures, Rb and N, in their aggregate state at a given pressure and temperature. The reference structures of elemental N and Rb used to calculate the enthalpy of formation are $\alpha\text{-N}_2$ and bcc Rb at 0 GPa, $\epsilon\text{-N}_2$ and $I4/m\bar{m}$ Rb at 30 GPa, and cg-N and $Cmca$ Rb at 60 GPa and 100 GPa. As the reference structures are not the focus of this paper and their phase diagrams are well known, pure Rb and N were not included in this USPEX search. The correct phases of rubidium have been predicted at high pressures using the USPEX algorithm²⁶ while a similar

method was used by C.J. Pickard and R. J. Needs³² to discover both experimentally known phases of nitrogen as well as new phases.

First-principles calculations are performed using DFT code VASP³³ and employing Perdew-Burke-Ernzerhof (PBE) generalized gradient approximation (GGA) to DFT³⁴, projector augmented wave (PAW) pseudopotentials, plane wave basis set with 350 eV energy cutoff, and k-point sampling with density 0.07 \AA^{-3} . For each pressure, the lowest enthalpy structures and those close to the convex hull are then calculated at higher accuracy to compute the true convex hulls. As triply-bonded nitrogen has extremely small bond lengths, the hard nitrogen PAW pseudopotential with the core radius 0.582 \AA is used. Correspondingly, the energy cutoff for the high accuracy calculations is raised to 1000 eV, while the k-point density is increased to 0.04 \AA^{-3} . The chemical bonding (atomic charges and the bond orders) in novel rubidium polynitrogen compounds is analyzed using local combination of atomic orbitals (LCAO) code DMol^{35,36}. The off-resonant Raman frequencies are obtained within frozen phonon approximation by calculating phonons at the gamma point, and their intensities – by calculating the derivatives of macroscopic dielectric polarizability tensor along the normal mode eigenvectors^{37,38}.

III. RESULTS AND DISCUSSION

Our first-principles structure search of Rb_xN_y compounds of varying stoichiometry produced several new rubidium polynitrogen structures at various pressures. The thermodynamically stable structures discovered in the search are displayed in the convex hulls (Fig. 1a) which are then used to produce the corresponding phase diagram (Fig. 1b). The crystal structures of several newly predicted Rb_xN_y compounds are shown in Fig. 2.

At 0 GPa, there are two stable compounds: RbN_2 - $P-1$ consisting of N_2 molecules (Fig. 2a) and Rb atoms, as well as experimentally known rubidium azide (RbN_3) polymorph with $I4/m\bar{m}$ symmetry (Fig. 2b)³⁹. These two compounds, RbN_2 and RbN_3 , remain stable at 15 GPa, RbN_3 transforming to the $C2/m$ phase and eventually becoming metastable at pressures above 30 GPa. This study correctly predicts the RbN_3 - $I4/m\bar{m}$ phase to be the most energetically favorable at ambient conditions³⁹, as well as the pressure-induced phase transition of this phase to that of $C2/m$ symmetry⁴⁰ in agreement with experiment. The validation of the USPEX method in the scope of this work is demonstrated by the correct prediction the RbN_3 phases listed above.

Wang *et al.*⁴¹ found that RbN_3 undergoes the following phase transitions: to a $P-1$ phase containing infinite chains of nitrogen at 30 GPa, and to $P6/mmm$ phase containing N_6 hexazine rings at 50 GPa. This is not what we found in this work. At 30 GPa, the lowest enthalpy structure is still the $C2/m$ phase. The $P6/mmm$ phase is not on the convex hull at 60 GPa, see corresponding open

violet circle in Figure 1a). Eventually, upon increasing pressure to 100 GPa, the $P6/mmm$ phase of RbN_3 with 6-membered hexazine rings becomes stable.

Several other structures appear above 15 GPa. One of them, Rb_3N_3 - $P-1$ crystal with 1:1 stoichiometry, consisting of bent N_3 chains and three Rb atoms per each N_3 molecule (Fig. 2c), remains the lowest formation enthalpy compound at pressures up to 38.4 GPa where it transforms to Rb_4N_4 - $P-1$ crystal with the same 1:1 stoichiometry containing one-dimensional four-atom nitrogen chains (N_4) and isolated Rb atoms, see Fig. 2d).

A phase diagram for the phases with 1:1 stoichiometry is constructed to predict the interval of pressures where the novel Rb_3N_3 - $P-1$ compound is stable. The three lowest RbN phases found during the USPEX search, Rb_3N_3 - $P-1$, Rb_4N_4 - $P-1$, Rb_2N_2 - $P-1$ - a , as well as an-

other high-pressure polymorph Rb_2N_2 - $P-1$ - b , were optimized at fixed pressures in interval from 0 to 100 GPa. The Rb_2N_2 - $P-1$ - b crystal has the same symmetry $P-1$, as Rb_2N_2 - $P-1$ - a , but has different positions of the nitrogen atoms. The reference structure for the compression analysis is taken to be the Rb_3N_3 - $P-1$ phase. As seen from Fig. 3, the Rb_2N_2 - $P-1$ - a phase, containing N_2 molecules and Rb atoms, is the lowest enthalpy phase only until 1.3 GPa. At 0 GPa, Rb_2N_2 - $P-1$ - a is 90 meV above the convex hull (1b)). From 1.3 GPa to 38.4 GPa the Rb_3N_3 - $P-1$ phase with the bent N_3 molecules, see Fig. 2c), is the lowest enthalpy phase. At pressures above 38.4 GPa the Rb_4N_4 - $P-1$ phase, consisting of bent N_4 molecules, is the lowest enthalpy phase, Fig. 2d).

On the rubidium-rich side of the convex hull, Rb_3N_2 - $C2/c$ and Rb_3N - $Pnma$ crystals are predicted to be stable at pressures above 15 GPa. They are composed of N_2 molecules and isolated Rb atoms. On the nitrogen-rich side, RbN_5 - Pc also appears on the convex hull at 15 GPa, which contains cyclo- N_5^- pentazole- five-member rings of nitrogen atoms (Fig. 2f)). This phase of RbN_5 remains the lowest stable phase at pressures up to 60 GPa, above this pressure it transforms to RbN_5 - $Pnma$.

At 60 GPa there is a phase transition of the RbN_2 crystal from the $P-1$ phase to the $Pbcn$ phase. This new phase, RbN_2 - $Pbcn$, consists of infinite chains of nitrogen atoms (Fig. 2g). Another compound predicted in this study, Rb_4N_6 - $P-1$ (Fig. 2h)), is close to the convex hull at 30 GPa, then appears on the convex hull at 60 GPa and remains stable to at least 100 GPa. This crystal, consisting of six-membered hexazine rings and having 4:6 stoichiometry, has analog in the family of cesium and potassium poly-nitrides: Cs_4N_6 becomes thermodynamically stable at pressures greater than 30 GPa and K_4N_6 becomes thermodynamically stable at pressures greater than 60 GPa.^{12,18}, but such stoichiometry has not been seen in the sodium¹³ or lithium studies¹⁷. However, in the latter case, as well as in case of Cs, the compound of different stoichiometry has been found to contain hexazine N_6 rings: LiN_3 above 60 GPa¹⁷, and CsN_3 from 80 GPa to at least 100 GPa¹⁶.

The prediction of RbN_5 adds this pentazolate compound to the list of other alkali pentazolates: LiN_5 ¹⁷, NaN_5 ¹³, CsN_5 ^{12,16}, and KN_5 ¹⁸. Therefore, an important conclusion can be made: XN_5 pentazolate crystals are the general feature of nitrogen-alkali metal chemistry at high pressures. The RbN_5 - Pc phase becomes stable at relatively low pressure of 15 GPa, which is similar to the case of three other alkali-pentazolate compounds: CsN_5 - stable at 15 GPa^{12,17}, LiN_5 - at 15 GPa¹⁷, KN_5 - stable at 15 GPa¹⁸ and NaN_5 - at 20 GPa¹³. In addition to pentazolates, infinite nitrogen chains are found in high pressure phase of RbN_2 - $Pbcn$, which was also seen in case of sodium, cesium, and lithium polynitrides. The infinite chain structure of RbN_2 in the $Pbcn$ phase exists at pressures greater than 60 GPa.

To understand the structure and bonding in the novel Rb_xN_y compounds, their charges and bond orders are

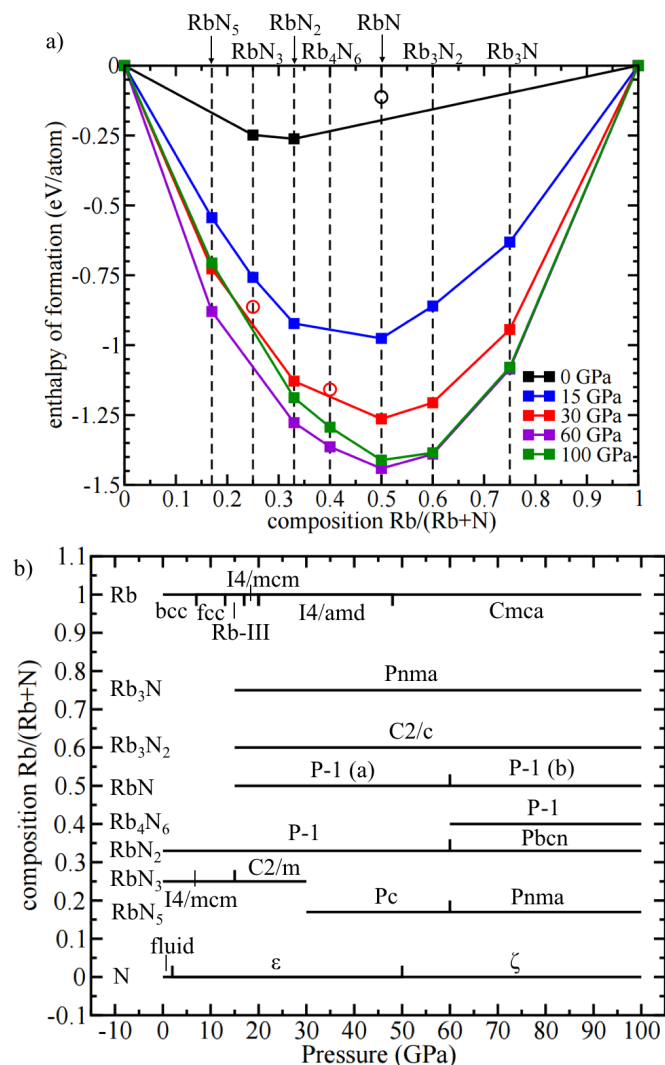


FIG. 1. a) Convex hulls at pressures 0, 15, 30, 60, and 100 GPa. Thermodynamically stable structures are marked by filled circles; metastable structures are marked with open circles. b) Composition versus pressure phase diagram of Rb_xN_y crystals.

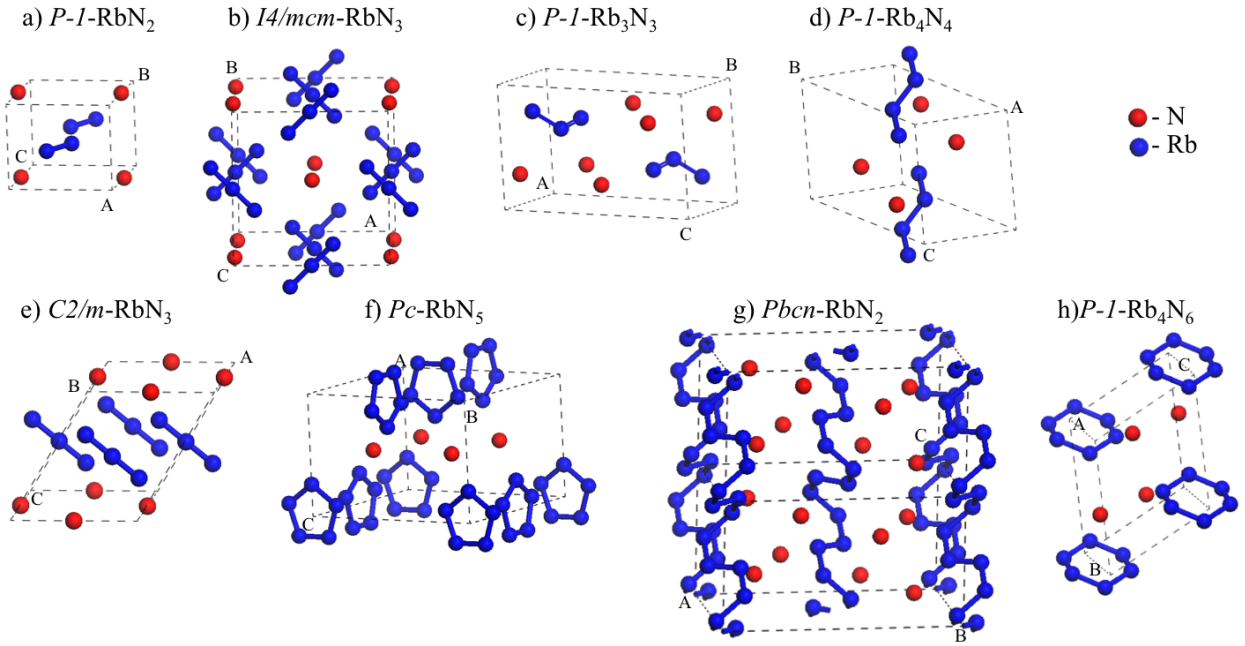


FIG. 2. Crystal structures of select rubidium polynitrides: a) RbN_2 -*P-1* (stable at 0-30 GPa); b) RbN_3 -*I4/mcm* (stable at 0-15 GPa); c) RbN -*P-1* (stable at 30-60 GPa); d) RbN -*P-1* (stable above 60 GPa); e) RbN_3 -*C2/m* (stable at 15-30 GPa); f) RbN_5 -*Pc* (stable at 30-60 GPa); g) RbN_2 -*Pbcn* (stable above 60 GPa); h) Rb_4N_6 -*P-1* (stable above 60 GPa)

calculated at 0 GPa and shown in Fig. 4. The N_2 molecules in RbN_2 -*P-1* crystal carry a net charge of $-0.248e$ and have the N-N bond order of 2.05, which indicates a double bond. At ambient conditions the bond order for the azide in rubidium azide (RbN_3) is 1.97 while the charge on both outer N atoms of the azide is $-0.508e$ and the charge on the center atom is $+0.397e$. The average bond order of the N-N bond in bent N_3 azides

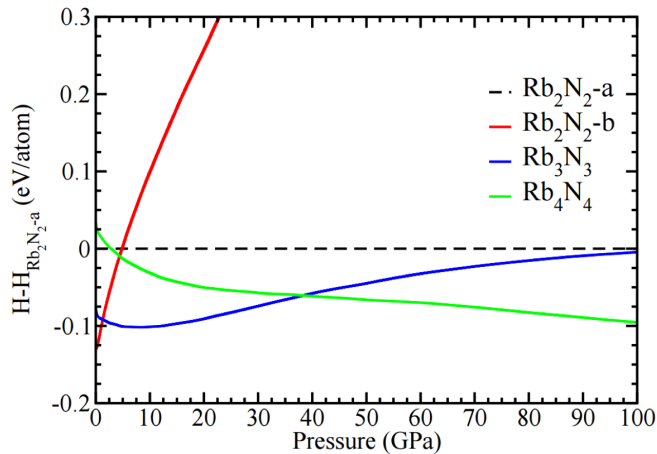


FIG. 3. Enthalpy difference between Rb_3N_3 -*P-1* phase and other phases of crystals with RbN stoichiometry (Rb_2N_2 -*P-1*-a from the 0 GPa search, Rb_2N_2 -*P-1*-b phase transition found during the compression study, and Rb_4N_4 -*P-1* from the 60 GPa search) showing where each phase is thermodynamically favorable.

in Rb_3N_3 -*P-1* crystal (which is stable above 60 GPa) is 1.32, see Fig. 3. The smaller bond order compared to the double N-N bonds (bond order 2) of N_3 azide in RbN_3 -*I4/mcm* is due to the filling of the anti-bonding orbitals by extra negative charge (the charge on the azide N_3 chain in RbN_3 -*I4/mcm* is -0.619 compared to -1.305 in Rb_3N_3 -*P-1*). The lowest enthalpy phase of RbN between 60 and 100 GPa, Rb_4N_4 -*P-1*, consists of bent N_4 molecules. The bond order of the N-N bonds in Rb_4N_4 -*P-1* crystal involving the outer N atom, carrying $-0.621e$, and the inner nitrogen atom, carrying the charge $-0.253e$, is 1.17 and the bond order of the bond between the two inner nitrogen atoms is 1.04. The charges on the nitrogen atoms in the cyclo- N_5 ring of the RbN_5 -*Pc* compound are $-0.171e$, $-0.121e$, $-0.182e$, $-0.167e$, and $-0.156e$ and the corresponding N-N bond orders range from 1.39 to 1.43, which demonstrates the aromatic nature of the pentazolate N_5^- anion.

The infinite N-N chains in RbN_2 -*Pbcn* crystal (the lowest enthalpy phase above 60 GPa), have varying N-N bond orders from 0.99 to 1.35. The charges on N atoms follow a cyclic pattern with two N atoms having charge of $-0.156e$ while the next two nitrogen atoms $-0.335e$ followed by two more nitrogen atoms of charge $-0.156e$ and so on. The irregular geometry of the nitrogen chains and the proximity of the nitrogen atoms to the rubidium atoms results in such irregular charge distribution.

The Rb_4N_6 -*P-1* phase, which is thermodynamically stable at pressures exceeding 60 GPa, contains N_6 hexazine rings. These rings are made of symmetric groups of three nitrogen atoms with bond orders of 1.03, 1.05,

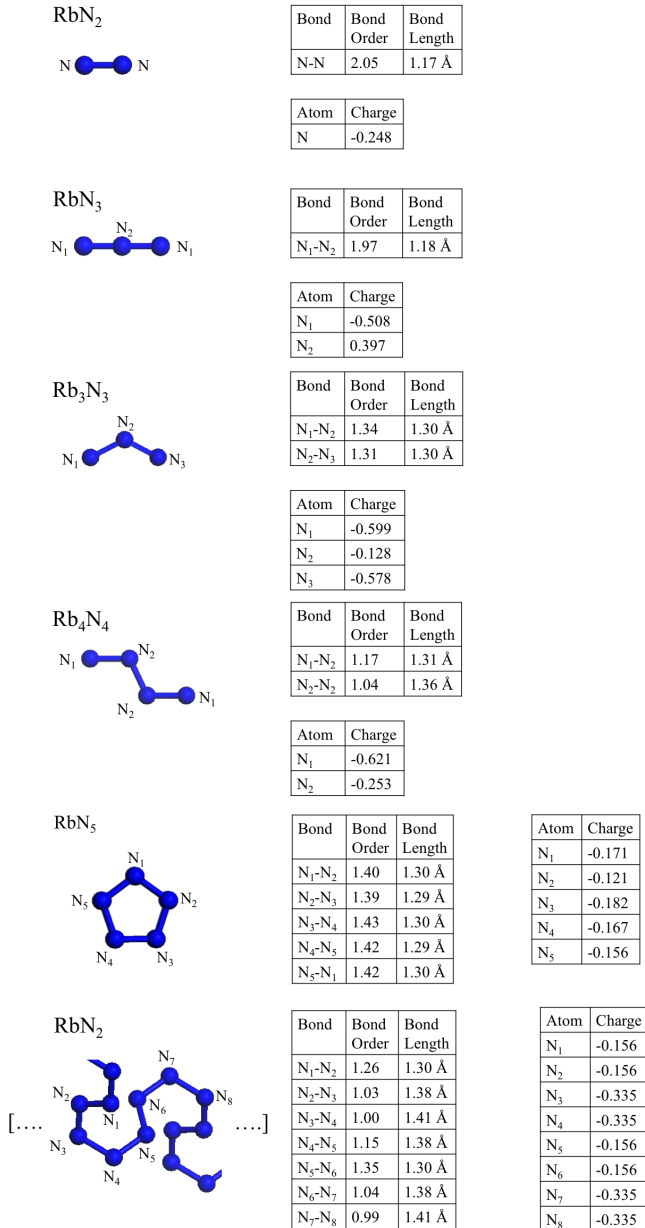


FIG. 4. Charges on the nitrogen atoms and the N-N bond orders for several Rb_xN_y crystals calculated at 0 GPa.

and 1.02, with nearly identical bond lengths of 1.41 Å between N₁-N₂ and 1.4 Å between N₂-N₃ and N₃-N₄. The charges on N atoms in N₆ ring vary from -0.344e to -0.371e.

The most nitrogen-rich compound, RbN₅ consisting of cyclo-N₅ pentazoles, can in principle be synthesized at high pressures by compressing rubidium azide (RbN₃) and nitrogen (N₂) mixture in a diamond anvil cell. Rubidium azide is well studied with several known phase transitions^{40–42}. To investigate whether synthesis can be achieved at modest pressures, the enthalpy difference between the phases of RbN₅ and precursors RbN₃-C2/m + N₂-R-3c is calculated as a function of pressure and shown

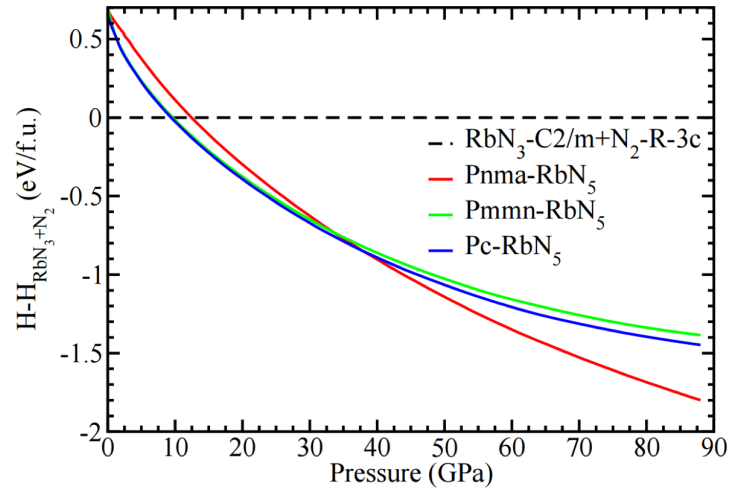


FIG. 5. Enthalpy difference between various phases of RbN₅ and the stoichiometric mixture of the precursors RbN₃ + N₂.

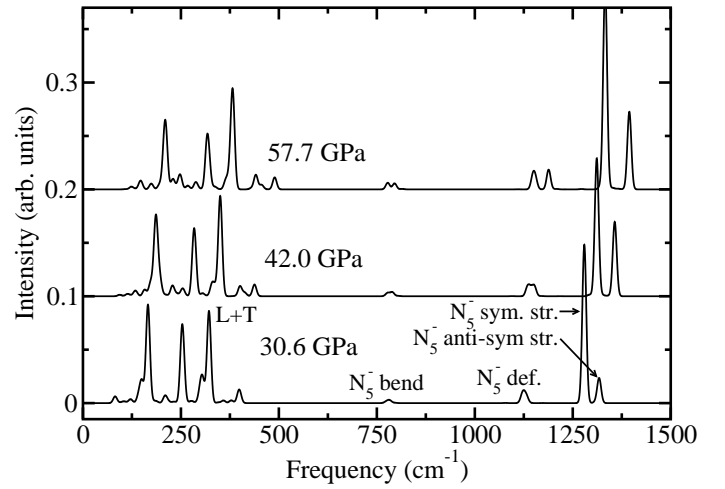


FIG. 6. The calculated Raman spectra of RbN₅-Pnma from 30.6 GPa up to 57.7 GPa. Mode assignments are given at 30.6 GPa, which show lattice and librational modes (L + T), N₅⁻ bending modes, N₅⁻ deformation (def.) modes, and N₅⁻ stretching (str.) modes.

in Fig. 5. As RbN₅-Pc is thermodynamically stabilized with respect to the precursors at 9.42 GPa, it can be synthesized upon compression above this pressure. Also seen from Fig. 5, RbN₅-Pc phase undergoes a phase transition to RbN₅-Pnma phase at 37.9 GPa, the latter being found in molecular search at 60 GPa.

As our work indicates a possibility of synthesis of RbN₅ upon compression of the mixture of rubidium azide RbN₃ and nitrogen N₂ precursors upon compression above 9.42 GPa, we calculated the pressure-dependent Raman spectra of RbN₅-Pnma phase from 30.6 GPa up to 57.7 GPa to assist in experimental identification of pentazoles, see Fig. 6. CsN₅ was successfully synthesized upon compressing and laser heating the precursors to pressures near 60 GPa¹². Due to the chemical similarities of Cs

and Rb, it is likely that synthesis of RbN_5 might occur under similar conditions of pressures high enough to provide additional PV enthalpy contribution to stimulate the chemical transformation. Due to this reason, the Raman spectrum of RbN_5 - $Pnma$ phase, the lowest formation enthalpy pentazolate phase at higher pressures, is calculated and shown in Fig. 4. The low frequency region in the Raman spectrum at 30.6 GPa from 85 to 401 cm^{-1} contains the lattice and N_5^- librational modes (L + T). Although there are several other librational modes in this region, three of them stand out due to their strong intensity at 166 cm^{-1} , 253 cm^{-1} , and 322 cm^{-1} , see Fig. 6. In addition, there are several N_5^- bending Raman modes with weak intensity at 781 cm^{-1} at 30.6 GPa. However, these modes split at higher pressures into two clearly visible bands at 778 cm^{-1} and 795 cm^{-1} at 57.7 GPa. Another mode splitting is found at higher pressures for the N_5 deformational (def.) band at 1125 cm^{-1} at 30.6 GPa, which splits into two clearly visible bands at 1151 cm^{-1} and 1189 cm^{-1} at 57.7 GPa. The two highest frequency bands are made of symmetry (sym.) and anti-symmetric breathing or stretching (str.) modes as seen in Fig. 6. All the calculated modes show normal pressure behavior with increasing pressure: the mode frequencies blue shift and their character does not change upon compression.

IV. CONCLUSION

Three novel high-nitrogen content Rb_xN_y compounds are discovered using first principles evolutionary structure search. The first, rubidium pentazolate RbN_5 - Pc consisting of cyclo- N_5^- anions is predicted to be thermodynamically stable at pressures exceeding 15 GPa. Heating and compressing the mixture of rubidium azide RbN_3 and N_2 gas is expected to produce RbN_5 as our calculations demonstrate that RbN_5 - Pc becomes thermodynamically preferred compared to the stoichiometric mixture of the precursors at pressures above 9.42 GPa. Raman spectrum of rubidium pentazolate RbN_5 - $Pnma$ is calculated to assist in experimental identification of N_5^- modes, which should be observed in experiment if such compound appears upon its synthesis. The second high-nitrogen content compound, RbN_2 - $Pbcn$, consisting of single bonded infinite nitrogen chains becomes thermodynamically stable at 60 GPa. The third newly discovered compound, Rb_4N_6 - $P-1$, consists of N_6 hexazine rings is thermodynamically stable at 60 GPa. In addition, a compound Rb_3N_3 - $P-1$ consisting of bent N_3 molecules, is predicted to be stable between 30 and 60 GPa. Although there are some similarities in structures of Rb polynitrogens with those found for other alkali polynitrides, the N_3 anions in Rb_3N_3 - $P-1$ phase have not been seen before.

ACKNOWLEDGMENTS

The research is supported by the Defense Threat Reduction Agency, (grant No. HDTRA1-12- 1-0023) and Army Research Laboratory through Cooperative Agreement W911NF-16-2-0022. Simulations were performed using the NSF XSEDE supercomputers (grant No. TG-MCA08X040), DOE BNL CFN computational user facility, and USF Research Computing Cluster supported by NSF (grant No. CHE-1531590).

REFERENCES

- ¹R. P. Singh, R. D. Verma, D. T. Meshri, and J. M. Shreeve, *Angew. Chemie Int. Ed.* **45**, 3584 (2006).
- ²T. M. Klapötke, in *High Energy Density Mater.*, Vol. 125 (Springer Berlin Heidelberg, Berlin, Heidelberg, 2007) pp. 85–121.
- ³G. Steinhauser and T. M. Klapötke, *Angew. Chemie Int. Ed.* **47**, 3330 (2008).
- ⁴M. Talawar, R. Sivabalan, T. Mukundan, H. Muthurajan, A. Sikder, B. Gandhe, and A. S. Rao, *J. Hazard. Mater.* **161**, 589 (2009).
- ⁵V. E. Zarko, *Combust. Explos. Shock Waves* **46**, 121 (2010).
- ⁶T. Brinck, *Green Energ. Mater.*, edited by T. Brinck (John Wiley & Sons, Ltd, Chichester, United Kingdom, 2014) pp. 1–290.
- ⁷M. I. Eremets, A. G. Gavriliuk, I. A. Trojan, D. A. Dzivenko, and R. Boehler, *Nat. Mater.* **3**, 558 (2004).
- ⁸M. I. Eremets, A. G. Gavriliuk, N. R. Serebryanaya, I. A. Trojan, D. A. Dzivenko, R. Boehler, H. K. Mao, and R. J. Hemley, *J. Chem. Phys.* **121**, 11296 (2004).
- ⁹C. Mailhot, L. H. Yang, and A. K. McMahan, *Phys. Rev. B* **46**, 14419 (1992).
- ¹⁰D. Tomasino, M. Kim, J. Smith, and C.-S. Yoo, *Phys. Rev. Lett.* **113**, 205502 (2014).
- ¹¹M. I. Eremets, I. A. Trojan, A. G. Gavriliuk, and S. A. Medvedev, *Static Compression Energ. Mater.*, edited by S. M. Peiris and G. J. Piermarini (Springer Berlin Heidelberg, Berlin, Heidelberg, 2008) pp. 75–97.
- ¹²B. A. Steele, E. Stavrou, J. C. Crowhurst, J. M. Zaug, V. B. Prakapenka, and I. I. Oleynik, *Chem. Mater.* **29**, 735 (2017).
- ¹³B. A. Steele and I. I. Oleynik, *Chem. Phys. Lett.* **643**, 21 (2016).
- ¹⁴B. A. Steele and I. I. Oleynik, *J. Phys. Chem. A* **121**, 1808 (2017).
- ¹⁵G. Vaitheeswaran and K. R. Babu, *J. Chem. Sci.* **124**, 1391 (2012).
- ¹⁶F. Peng, Y. Han, H. Liu, and Y. Yao, *Sci. Rep.* **5**, 16902 (2015).
- ¹⁷Y. Shen, A. R. Oganov, G. Qian, J. Zhang, H. Dong, Q. Zhu, and Z. Zhou, *Sci. Rep.* **5**, 14204 (2015).
- ¹⁸B. A. Steele and I. I. Oleynik, *J. Phys. Chem. A* (2017), DOI:10.1021/acs.jpca.7b08974.
- ¹⁹M. T. Nguyen and T.-K. Ha, *Chem. Phys. Lett.* **335**, 311 (2001).
- ²⁰A. Vij, J. G. Pavlovich, W. W. Wilson, V. Vij, and K. O. Christe, *Angew. Chemie - Int. Ed.* **41**, 3051 (2002).
- ²¹C. Zhang, C. Yang, B. Hu, C. Yu, Z. Zheng, and C. Sun, *Angew. Chemie Int. Ed.* **56**, 4512 (2017).
- ²²C. Zhang, C. Sun, B. Hu, C. Yu, and M. Lu, *Science* (80-.). **355**, 374 (2017).
- ²³B. Bazanov, U. Geiger, R. Carmieli, D. Grinstein, S. Welner, and Y. Haas, *Angew. Chemie Int. Ed.* **55**, 13233 (2016).
- ²⁴Y. Xu, Q. Wang, C. Shen, Q. Lin, P. Wang, and M. Lu, *Nature* **549**, 78 (2017).
- ²⁵U. Schwarz, A. Grzechnik, K. Syassen, I. Loa, and M. Hanfland, *Phys. Rev. Lett.* **83**, 4085 (1999).
- ²⁶Y. Ma, A. R. Oganov, and Y. Xie, *Phys. Rev. B* **78**, 014102 (2008).

- ²⁷M. Hanfland, I. Loa, and K. Syassen, *Phys. Rev. B* **65**, 184109 (2002).
- ²⁸C. W. Glass, A. R. Oganov, and N. Hansen, *Comput. Phys. Commun.* **175**, 713 (2006).
- ²⁹A. R. Oganov and C. W. Glass, *J. Chem. Phys.* **124**, 244704 (2006).
- ³⁰A. O. Lyakhov, A. R. Oganov, and M. Valle, *Comput. Phys. Commun.* **181**, 1623 (2010).
- ³¹A. Hermann (John Wiley & Sons, Inc., 2017) pp. 1–41.
- ³²C. J. Pickard and R. J. Needs, *Phys. Rev. Lett.* **102**, 125702 (2009).
- ³³G. Kresse and J. Furthmüller, *Comput. Mater. Sci.* **6**, 15 (1996).
- ³⁴J. P. Perdew, K. Burke, and M. Ernzerhof, *Phys. Rev. Lett.* **77**, 3865 (1996).
- ³⁵B. Delley, *J. Chem. Phys.* **92**, 508 (1990).
- ³⁶B. Delley, *J. Chem. Phys.* **113**, 7756 (2000).
- ³⁷M. Lazzeri and F. Mauri, *Phys. Rev. Lett.* **90**, 036401 (2003).
- ³⁸D. Porezag and M. R. Pederson, *Phys. Rev. B* **54**, 7830 (1996).
- ³⁹D. Li, X. Wu, J. Jiang, X. Wang, J. Zhang, Q. Cui, and H. Zhu, *Appl. Phys. Lett.* **105**, 071903 (2014).
- ⁴⁰D. Li, F. Li, Y. Li, X. Wu, G. Fu, Z. Liu, X. Wang, Q. Cui, and H. Zhu, *J. Phys. Chem. C* **119**, 16870 (2015).
- ⁴¹X. Wang, J. Li, N. Xu, H. Zhu, Z. Hu, and L. Chen, *Sci. Rep.* **5**, 16677 (2015).
- ⁴²W. Zhu, J. Xiao, and H. Xiao, *J. Phys. Chem. B* **110**, 9856 (2006).